INTERNATIONAL JOURNAL FOR NUMERICAL METHODS IN FLUIDS
Int. J. Numer. Meth. Fluids 2006; **50**:925–945
Published online 17 October 2005 in Wiley InterScience (www.interscience.wiley.com). DOI: 10.1002/fld.1088

On uniformly accurate high-order Boussinesq difference equations for water waves

Yaron Toledo*,† and Yehuda Agnon‡

Civil and Environmental Engineering, Technion, Haifa, Israel

SUMMARY

A new accurate finite-difference (AFD) numerical method is developed specifically for solving high-order Boussinesq (HOB) equations. The method solves the water-wave flow with much higher accuracy compared to the standard finite-difference (SFD) method for the same computer resources. It is first developed for linear water waves and then for the nonlinear problem. It is presented for a horizontal bottom, but can be used for variable depth as well. The method can be developed for other equations as long as they use Padé approximation, for example extensions of the parabolic equation for acoustic wave problems. Finally, the results of the new method and the SFD method are compared with the accurate solution for nonlinear progressive waves over a horizontal bottom that is found using the stream function theory. The agreement of the AFD to the accurate solution is found to be excellent compared to the SFD solution. Copyright © 2005 John Wiley & Sons, Ltd.

KEY WORDS: Boussinesq methods; nonlinear waves; accurate numerical methods; coastal and offshore engineering

1. INTRODUCTION

Accurate and efficient prediction of the nonlinear evolution of fully dispersive water-waves over a bathymetry poses a formidable challenge. In recent years, a large number of studies were devoted to models that are related to high-order Boussinesq (HOB) theory enhancing the original work by Boussinesq [1].

The irrotational flow of an incompressible homogeneous inviscid fluid is generally a three-dimensional problem. Boussinesq-type equations reduce the description to a two-dimensional one by introducing a polynomial approximation to the vertical distribution of the flow into integral conservation laws, while accounting for non-hydrostatic effects due to the vertical acceleration (see Reference [2]). A number of variants exist. These have computational complexities proportional to the area of the free surface (and to the order of the model), which

*Correspondence to: Yaron Toledo, Civil and Environmental Engineering, Technion, Haifa, Israel.
†E-mail: yaront@tx.technion.ac.il
‡E-mail: agnon@tx.technion.ac.il

Received 8 May 2005
Revised 10 August 2005
Accepted 14 August 2005

makes them very attractive. In general, HOB models have an algebraic dispersion relation, which approximates the exact (transcendental) dispersion relation of the fully dispersive water-waves theory.

The accuracy of these approximate dispersion relations, decreases with the increasing of the relative water depth, kh (h—water depth, k—wavenumber). The accuracy of the models also decreases with the increasing of the nonlinearity parameter H/h (H—wave height). Finally, the models' accuracy decreases with the increase of bottom depth variations (e.g. bottom slope steepness). The errors decrease as the order of the models is increased.

There are several ways to arrive at HOB models. The various HOB theories, derived in different ways, typically share similar dispersion characteristics, for equivalent model order. They differ among themselves in their nonlinear characteristics.

The dispersion relations in HOB models express the wave's frequency-squared, as even rational functions of its wavenumber. Many versions of HOB theory yield expressions in the form of Padé Approximants. These produce a good representation of the dispersion relation $\omega^2 = gk \tanh(kh)$, from $kh = 0$, past the radius of convergence of its Taylor series (g—gravity).

The error in the approximation of the dispersion relation increases with kh. Although the accuracy increases with the order of the method, the deep water limit, $\omega^2 = gk$ cannot be attained by an even function of k. An exception to this is the Fourier–Boussinesq method [3], which successfully approaches the dispersion relation from shallow water to deep water.

In general the derivations are based on assuming a polynomial velocity profile at each vertical transect. The simplest model of this type is 'Shallow Water Theory', in which the velocity has no variation along the vertical axis. Next come the classic Boussinesq equations (and the Korteweg–deVries (KdV) Equation, which possesses soliton solutions) with a parabolic profile. Higher in this hierarchy are the various order HOB models (see Reference [4]).

HOB models can be derived in several ways: by using as variables the velocities at intermediate depths (see Reference [5]), by enhancement of the equations through operational calculus (see Reference [6]), by local polynomial methods (see Reference [7]), by two layer models (see Reference [8]), or using an auxiliary potential (see Reference [9]).

Several models introduce auxiliary variables, e.g. by dividing the fluid domain into sub-layers, or by expanding the velocity profile into a sum of basis functions. The overall order of the model is effectively the product of the order of each variable, times the number of variables. Thus, a trade off is in effect.

Extensions of HOB models incorporate wave–current interaction, wave–body interaction, wave-breaking and dissipation. For reviews see References [4, 10].

All the above progress is related to the development of the analytical equations of Boussinesq-type models. However, in order to solve these equations for realistic problems we usually write the numerical approximation of these equations, apply them to a geometrical grid and solve the resulting set of linear equations for a specific problem. This method of solution (which is the most common) may reduce the accuracy of the already approximate Boussinesq equations. One of the wide spread numerical methods is the finite-difference (FD) method. In this method the derivatives of a function (in our case the velocity potential or the free surface elevation) at a certain grid point are approximated using the numerical values of the function in the grid point and the neighbouring grid points to some range. The accuracy of the solution increases with the order of the method (the number of neighbouring grid points that interact with each other) and decreases with the grid size. The computational cost follows opposite trends. The FD method has not been optimized for solving Boussinesq-type equations.

Harari and Turkel [11] have developed high-order FD methods specifically for the Helmholtz equation that proved to be much more effective than the standard method. The goal of the present work is to merge the FD method with the Boussinesq concept in order to construct a new accurate FD (AFD) method specifically for Boussinesq-type equations and other similar differential equations. First, a new method will be constructed for the linear part and then the FD method will be extended along the lines of Agnon *et al.* [6] and Madsen and Agnon [12] in order to formulate a numerical method for nonlinear high-order Boussinesq-type equations.

The HOB analytical Dirichlet to Neumann (DtN) operator is presented in Section 2 with infinite order of accuracy using operational calculus. In Section 3 the differential operator (∇) is represented as a fully accurate difference operator, which combined with the analytical DtN operator yields an infinitely accurate difference representation of HOB. The new difference operator is then approximated using a Padé rational series to give a new AFD method. The accuracy of the AFD and the standard FD (SFD) methods are compared to the known linear analytical solution in Section 4. The AFD presents excellent behaviour and is found to be superior compared to the standard FD method. An extension of the AFD model to nonlinear waves is presented in Sections 5 and 6. The results of the two numerical methods are compared in Section 7 to the accurate solution for nonlinear progressive waves over a horizontal bottom, which is found using the stream function theory. Again, the results of the AFD are in better agreement with those of the accurate solution proving the new AFD method to be an improved alternative to the SFD method for nonlinear Boussinesq-type equations.

2. ELIMINATING THE VERTICAL COORDINATE

The equations governing the irrotational flow of an incompressible inviscid fluid with a free surface over a horizontal bottom are

$$\nabla^2\Phi + \Phi_{zz} = 0, \quad -h < z < \eta \tag{1}$$

$$\eta_t + \nabla\Phi\nabla\eta - \Phi_z = 0, \quad z = \eta \tag{2}$$

$$\Phi_t + \tfrac{1}{2}(\nabla\Phi)^2 + \tfrac{1}{2}(\Phi_z)^2 + g\eta = 0, \quad z = \eta \tag{3}$$

$$\Phi_z = 0, \quad z = -h \tag{4}$$

Here, Φ is the velocity potential, h is the water depth and η the surface elevation. The origin is on the undisturbed water level and z is positive upward. The horizontal gradient operator relates Φ to the horizontal velocity, $\mathbf{u}$:

$$\mathbf{u} = (u, v) = \nabla\Phi, \quad \nabla = \left(\frac{\partial}{\partial x}, \frac{\partial}{\partial y}\right) \tag{5}$$

For convenience we denote $\Phi_z = W$ and use the hat ($\hat{}$) and tilde ($\tilde{}$) signs to denote the value on $z = 0$ and on $z = \eta$, respectively. For completeness we give a short review of HOB derivation.

One of the main ideas of Boussinesq-type theories is to reduce the three-dimensional description to a two-dimensional one. The first step towards such a reduction is to introduce

an expansion of the velocity potential as a power series in the vertical coordinate:

$$\Phi(x,y,z,t)=\sum_{n=0}^{\infty}(z+h)^n\phi_n(x,y,t) \tag{6}$$

By substituting this expansion into (1) we find

$$\Phi(x,y,z,t)=\sum_{n=0}^{\infty}(-1)^n\left(\frac{(z+h)^{2n}}{(2n)!}\nabla^{2n}\phi_0+\frac{(z+h)^{2n+1}}{(2n+1)!}\nabla^{2n}\phi_1\right) \tag{7}$$

This is a series solution with two unknown functions ϕ_0 and ϕ_1. Note that the velocities at the undisturbed surface are given by

$$\hat{\mathbf{u}}=\nabla\hat{\Phi}=\nabla\phi_0,\quad \hat{W}=\phi_1 \tag{8}$$

Now by the use of (7) and (8) the horizontal bottom condition (4) can be expressed as

$$L_c\{\hat{W}\}+L_s\cdot\{\nabla\hat{\Phi}\}=0 \tag{9}$$

with

$$L_c=\sum_{n=0}^{\infty}(-1)^n\frac{h^{2n}}{(2n)!}\nabla^{2n},\quad L_s=\sum_{n=0}^{\infty}(-1)^n\frac{h^{2n+1}}{(2n+1)!}\nabla^{2n+1} \tag{10}$$

where ∇ is the gradient operator when applied to a scalar, and the divergence when applied to a vector. This equation defines a relation between $\hat{W}$ and $\hat{\Phi}$, which is of infinite order in $h\nabla$. The series are convergent if Φ has a Fourier transform, since they correspond to the analytic functions $\sinh(kh)$ and $\cosh(kh)$ where ik is the Fourier symbol of ∇.

Following Rayleigh [13], we may use symbolic notation of Taylor series operators by which (10) can be given in the compact form

$$L_c=\cos(h\nabla),\quad L_s=\sin(h\nabla) \tag{11}$$

so that (9) becomes

$$\cos(h\nabla)\hat{W}+\sin(h\nabla)\nabla\hat{\Phi}=0 \tag{12}$$

and (7) and its z derivative become

$$\Phi(x,y,z,t)=\cos(z\nabla)\hat{\Phi}+\frac{\sin(z\nabla)}{\nabla}\hat{W} \tag{13}$$

$$W(x,y,z,t)=-\sin(z\nabla)\nabla\hat{\Phi}+\cos(z\nabla)\hat{W} \tag{14}$$

Using (12) we can easily construct a DtN relation

$$\hat{W}=-\tan(h\nabla)\nabla\hat{\Phi} \tag{15}$$

and define the DtN operator as

$$G=-\tan(h\nabla)\nabla \tag{16}$$

Operator (16) is of infinite order yielding an accurate dispersion relation. Nevertheless, for practical use this operator needs to be approximated by a finite order representation. The

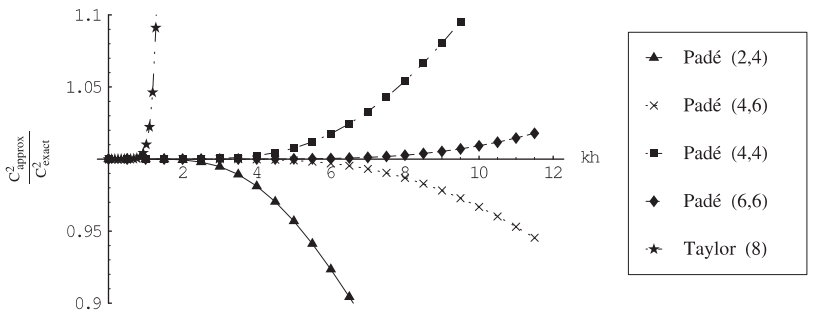

Figure 1. The accuracy of the linear dispersion relation for analytical Boussinesq-type equations of different approximations.

simplest way of doing so is by truncating the Taylor series representing the operator. The higher the order of derivatives kept in the Taylor expansions the higher is their accuracy. However, there is a better way to approximate this operator.

Padé approximation uses a ratio of two power series. It has double the accuracy of the Taylor approximation, while using the same order of derivatives. For example Taylor $(2n)$ represents the Taylor series up to $O(\nabla^{2n})$ (including) and Padé$(2n, 2n)$ represents the Padé approximation up to $O(\nabla^{4n})$. Note that the operator is even, therefore, for the Taylor approximation the lowest order term neglected is actually of $O(\nabla^{2n+2})$ and for the Padé approximation it is of $O(\nabla^{4n+2})$ using the same order of derivatives. Figure 1 shows the ratio between several approximations of the DtN operator (16) to its accurate form, which gives the analytical linear dispersion relation. We can see that Padé approximations agree much better with the analytical linear dispersion relation than the Taylor series.

After approximating the DtN operator we need to use a numerical method in order to practically solve the differential equation. A most common method for solving differential equations is the FD method. The main concept of this method is to replace a local derivatives with an approximation using the function values in nearby locations. The approximation used for that purpose is the Taylor series. As stated before this approximation is less efficient compared to the Padé approximation. When solving Boussinesq-type equations numerically approximations are made twice. First, using Padé approximation in order to develop the DtN relation to a requested order and second, using Taylor series in order to construct the relation as a set of algebraic equations. In the next section an infinite order FD derivative operator is combined with the DtN operator to be approximated together only once using Padé approximation. This results in a much more efficient method.

Madsen *et al.* [4] denote the HOB according the Padé approximation of: $-\tan(h\nabla)/h\nabla$. Although, we apply the Padé approximation to Equation (16), we keep the terminology of Madsen *et al.* For example, when Padé$(4,4)$ is applied to Equation (16) the corresponding terminology, Padé$(2,4)$, will be used.

3. CONSTRUCTING AN ACCURATE FD METHOD FOR THE LINEAR DIRICHLET TO NEUMANN RELATION

For convenience of presentation we chose to develop the approximation for one-dimensional distribution waves ($\nabla = \partial/\partial x$). The method is easily extended to two horizontal dimensions.

Using Taylor series we can define:

$$f\left(\frac{d}{2}\right) - f(0) = \frac{d}{2}\nabla f + \frac{d^2}{2^2 2!}\nabla^2 f + \cdots + \frac{d^n}{2^n n!}\nabla^n f + \cdots \tag{17}$$

$$f(0) - f\left(-\frac{d}{2}\right) = \frac{d}{2}\nabla f - \frac{d^2}{2^2 2!}\nabla^2 f + \cdots + (-1)^{n+1}\frac{d^n}{2^n n!}\nabla^n f + \cdots \tag{18}$$

Here, d is the constant length between grid points and f is an arbitrary function. Summing Equations (17) and (18) including all their terms and utilizing Rayleigh's notation yields

$$f\left(\frac{d}{2}\right) - f\left(-\frac{d}{2}\right) = 2\,\sinh\left(\frac{d}{2}\nabla\right) f \tag{19}$$

By defining a FD operator (δ) Equation (19) transforms to

$$\delta f = 2\,\sinh\left(\frac{d}{2}\nabla\right) f \tag{20}$$

Equation (20) defines the FD operator δ as an infinite power series of the differential operator ∇. This is equivalent to the Fourier representation of δ that is usually used in stability analyses. Solving this equation for ∇ allows us to represent it as a fully accurate FD operator

$$\nabla = \frac{2}{d}\,\mathrm{arcsinh}\left(\frac{\delta}{2}\right) \tag{21}$$

By substituting (21) into (16) we get a fully accurate FD definition of the DtN operator

$$G = -\frac{2}{d}\tan\left(\frac{2h}{d}\mathrm{arcsinh}\left(\frac{\delta}{2}\right)\right)\mathrm{arcsinh}\left(\frac{\delta}{2}\right) \tag{22}$$

Now all that is left to do in order to form a numerical stencil is to use an approximation to truncate the infinite FD operator G. Here, Padé$(2,4)$ is used as an example, but any other order of approximation is applicable (see Appendix A for Padé$(4,6)$),

$$\begin{aligned}\bar{\bar{A}}_p/\bar{\bar{B}}_p = {} & (-15(252d^6 + 1344d^2h^4)h\delta^2 - 15(31d^6 + 112d^2h^4 - 128h^6)h\delta^4)/ \\ & ((3780d^8 + 20160d^4h^4 + (780d^8 - 1260d^6h^2 + 3360d^4h^4 - 8640d^2h^6)\delta^2 \\ & + (23d^8 - 155d^6h^2 - 28d^4h^4 - 720d^2h^6 + 192h^8)\delta^4)\end{aligned} \tag{23}$$

We can now define the DtN relation (9) using (23) to get

$$\bar{\bar{B}}_p\hat{W} = \bar{\bar{A}}_p\hat{\Phi} \tag{24}$$

where $\bar{\bar{A}}_p$ and $\bar{\bar{B}}_p$ are the numerator and denominator presented in Equation (23), respectively, in their FD matrices form (see Appendix A for their stencils). In order to solve the linear wave problem we can use the set of linear equations presented in (24) for computing the vertical velocity $\hat{W}$. Then the problem can be marched in time using the linearized form of Equations (2) and (3).

4. COMPARING THE ACCURACY OF THE NEW ACCURATE FD METHOD TO THE STANDARD FD METHOD IN THE LINEAR PROBLEM

Since the linear water wave problem has an exact analytical solution and its dispersion relation is known, a comparison to numerical dispersion relations can be delineated analytically. The better a numerical stencil is, the better the agreement of its dispersion with the exact one. Both numerical methods, AFD and SFD should agree with the analytical dispersion relation only to a limited extent, even with a grid spacing that approaches zero. This arises from the fact that the Boussinesq equations are in essence approximate. When the grid spacing approaches zero, the numerical methods will never reach the genuine dispersion relation, but only an approximated one, which is derived from the specific Boussinesq equation that has been chosen (see Figure 1).

Note that the SFD method was used in its highest accuracy available for the same computational effort as the AFD method. For the AFD method, Padé$(2,4)$ and Padé$(4,6)$ indicates that band widths of 5 and 7 grid points are used. Therefore, the SFD method taken for comparison used all the grid points of the band even for lower derivatives in order to achieve its highest accuracy available for the same computational effort.

A Boussinesq equation using Padé$(2,4)$ gives a maximal dispersion ratio error of 2% when dealing with waves of $kh \simeq 4$ and less, where k is the wavenumber and h is the water depth. In principle, every numerical method further degrades the accuracy with respect to the grid spacing (d), therefore, if we accept a maximal dispersion ratio error of 2% the solution is expected to be limited by a smaller value of kh.

As we can see in Figure 2, when the grid spacing with respect to the wave length (kd) approaches zero the SFD method and the AFD method behave in the same way giving the dispersion relation of the analytical Padé$(2,4)$ HOB equation (shown in Figure 1). When kd is increased, we can see that the accuracy of the linear dispersion relation is rapidly decreasing for the standard FD method, whereas the new accurate FD method shows much

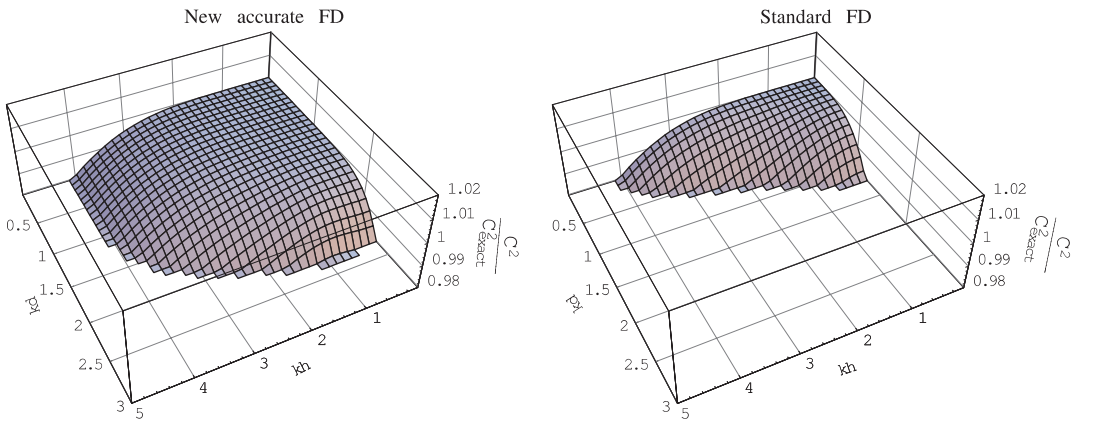

Figure 2. The ratio between the numerical linear dispersion relation and the exact analytical one for the new AFD method and the SFD method, while approximating the Padé$(2,4)$ HOB equation with respect to kh and kd.

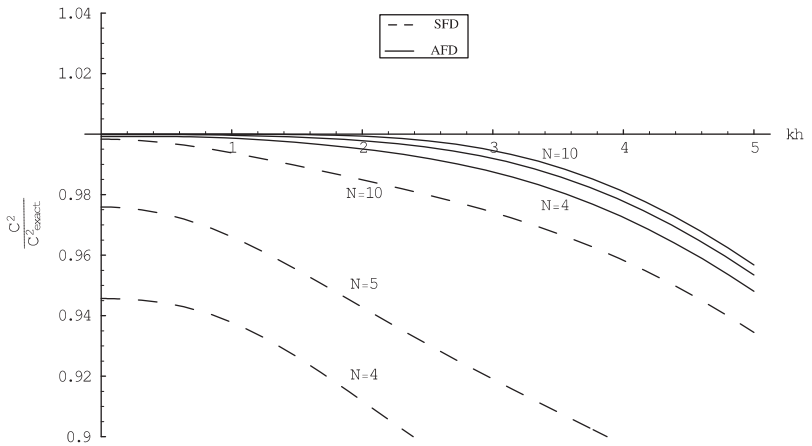

Figure 3. The ratio between the numerical linear dispersion relation and the exact analytical one for the new AFD method and the SFD method, while approximating the Padé(2,4) HOB equation with respect to kh for several values of grid points per wave length ($N = 2\pi/kd$). - - - SFD, —— AFD.

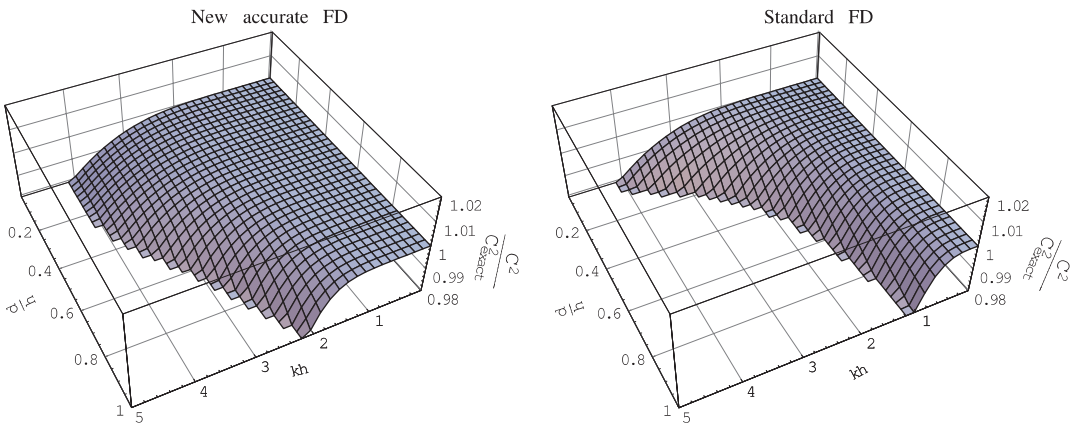

Figure 4. The ratio between the numerical linear dispersion relation and the exact analytical one for the AFD method and the SFD method, while approximating the Padé(2,4) HOB equation with respect to kh and d/h.

better behaviour. We can see that for 5 grid points per wave length and less ($kd \simeq 1.25$ and above) the SFD method cannot be used for the above error limit but, the AFD method enables us to solve for waves of up to $kh \simeq 3.9$, which means that there is almost no further loss of accuracy due to the AFD method, when we use a stencil of 5 or more grid points per wave length for the Padé(2,4) Boussinesq equation (Figure 3). In Figure 4 we can see that AFD method again demonstrates much better behaviour allowing calculation for larger kh with respect to any ratio of grid spacing to depth (d/h) under the same error limitations. Figure 5 describes the allowed $kh-kd$ region and $kh-d/h$ region for maximal dispersion ratio

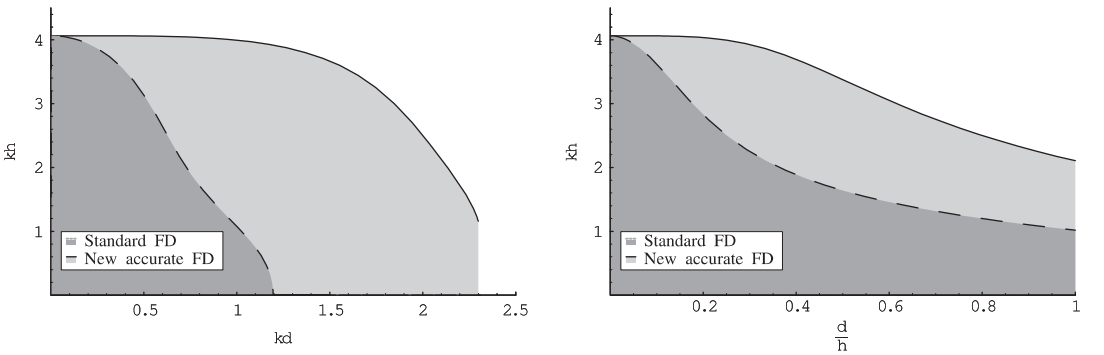

Figure 5. The allowed regions in each method for maximal dispersion ratio error of 2% while approximating the Padé(2, 4) HOB equation.

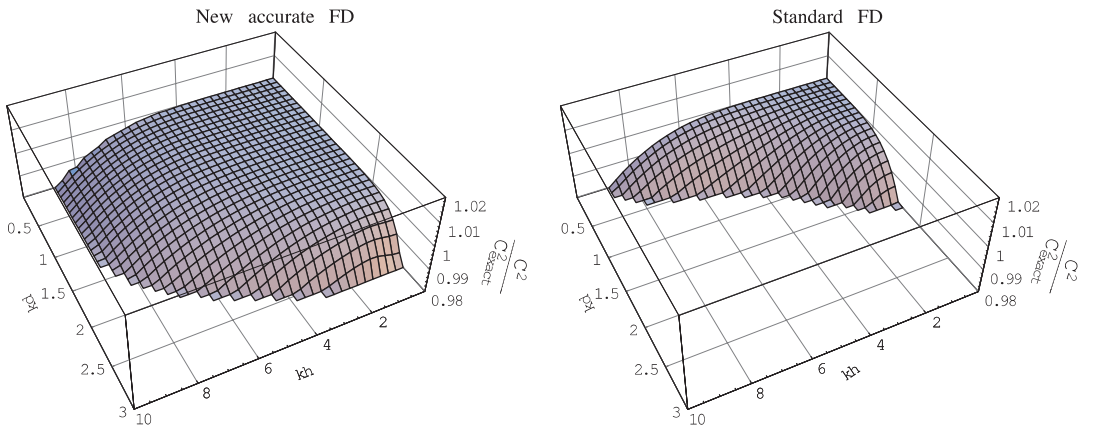

Figure 6. The ratio between the numerical linear dispersion relation and the exact analytical one for the new AFD method and the SFD method, while approximating the Padé(4, 6) HOB equation with respect to *kh* and *kd*.

error of 2%. As before, it is clear that the AFD method performs better than the SFD one. Similar results for the Padé(4, 6) Boussinesq equation are shown in Figures 6–9. As before, the new AFD method performs much better giving almost no decrease in accuracy for 4–5 and more grid points per wave length.

We can see that there is a significant increase in the capabilities of the AFD method with comparison to the SFD method in the linear case. Here we have regarded the benefits of the method for the first harmonic, but in the nonlinear case except for the increase in accuracy in the first harmonic there will be an increase in accuracy for higher harmonics as well. Even if we chose to work with finer grids for other reasons, such as calculations of breaking waves, for higher and higher harmonics we shall have lower and lower number of grid points per wave length resulting in a decrease in accuracy. Therefore, the AFD method benefits us in the nonlinear case as well, giving higher accuracy for the first and higher harmonics.

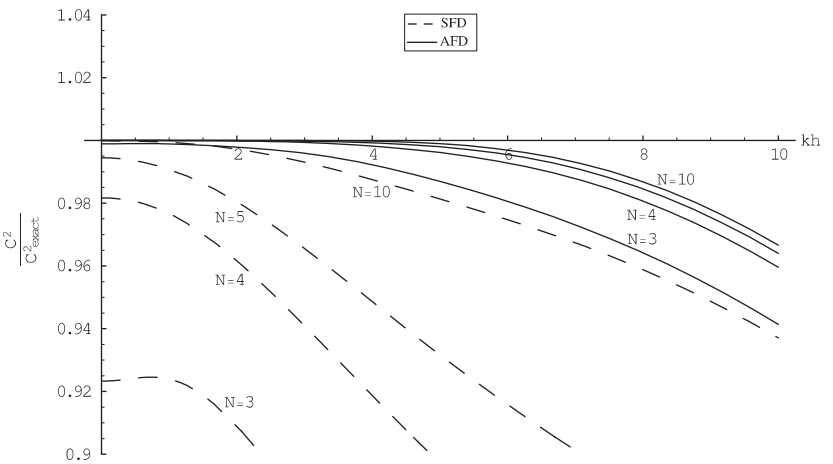

Figure 7. The ratio between the numerical linear dispersion relation and the exact analytical one for the new AFD method and the SFD method, while approximating the Padé(4, 6) HOB equation with respect to kh for several values of grid points per wave length ($N = 2\pi/kd$). - - - SFD, —— AFD.

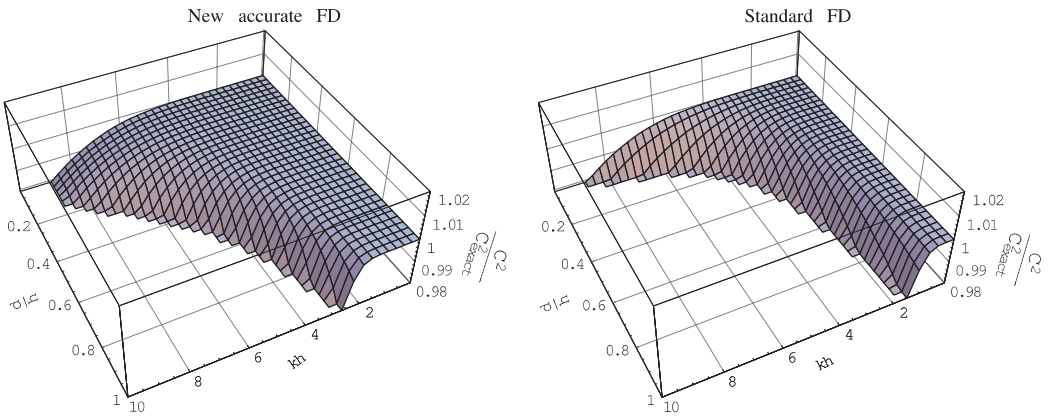

Figure 8. The ratio between the numerical linear dispersion relation and the exact analytical one for the new AFD method and the SFD method, while approximating the Padé(4, 6) HOB equation with respect to kh and d/h.

5. CONSTRUCTING AN ACCURATE FD METHOD FOR THE NONLINEAR DIRICHLET TO NEUMANN RELATION

An important motivation for using Boussinesq equations, except for the elimination of the vertical coordinate, is to be able to account for nonlinear effects. Therefore, the new accurate method should be extended to comprise nonlinearity. In 2003, Madsen and Agnon [12] have given a new formulation doubling the relative order of the vertical coordinates. We shall

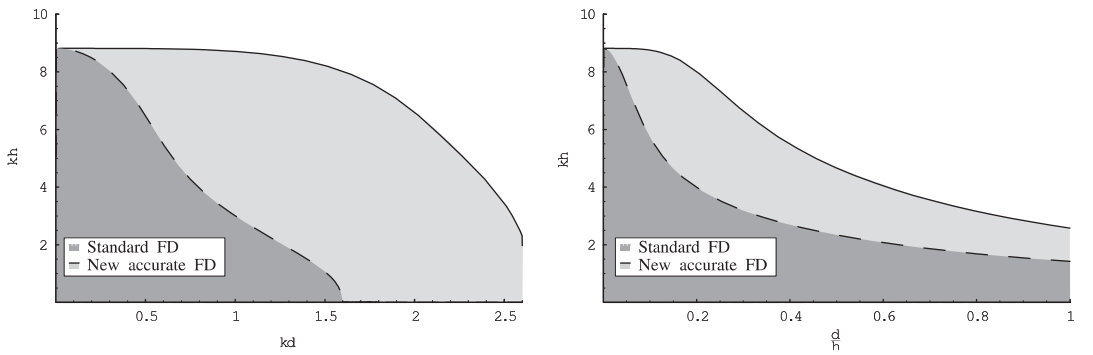

Figure 9. The allowed regions in each method for maximal dispersion ratio error of 2% while approximating the Padé(4,6) HOB equation.

implement the fully accurate FD operator on this new formulation and construct a DtN operator for nonlinear waves.

As stated in Equation (1), the velocity potential satisfies the Laplace equation. Furthermore, we can use the Laplace operator successively to replace horizontal differentiations by vertical ones to obtain

$$\nabla^{2m}\Phi = (-1)^m \frac{\partial^{2m}\Phi}{\partial z^{2m}} \tag{25}$$

Next we use Equation (20) to define even powers of the FD operator

$$\delta^{2m} = \left(2\,\sinh\left(\frac{d}{2}\nabla\right)\right)^{2m} \tag{26}$$

Notice that when we take the Taylor series of (26) all the powers of ∇ will be even and could be replaced using (25) with vertical derivatives to give

$$\begin{aligned}
\delta^2 &= d^2\frac{\partial^2}{\partial z^2} + \frac{d^4}{12}\frac{\partial^4}{\partial z^4} + \frac{d^6}{360}\frac{\partial^6}{\partial z^6} + \frac{d^8}{20160}\frac{\partial^8}{\partial z^8} + \frac{d^{10}}{1814400}\frac{\partial^{10}}{\partial z^{10}} + \cdots \\
\delta^4 &= d^4\frac{\partial^4}{\partial z^4} + \frac{d^6}{6}\frac{\partial^6}{\partial z^6} + \frac{d^8}{80}\frac{\partial^8}{\partial z^8} + \frac{17d^{10}}{30240}\frac{\partial^{10}}{\partial z^{10}} + \cdots
\end{aligned} \tag{27}$$

Again we utilize the expansion of the velocity potential as a power series in the vertical coordinates:

$$\begin{aligned}
\Phi(x,y,z,t) &= \sum_{n=0}^{N} (z+h)^n \phi_n(x,y,t) \\
W(x,y,z,t) &= \sum_{n=0}^{N} n(z+h)^{n-1} \phi_n(x,y,t)
\end{aligned} \tag{28}$$

which yields, for the vertical derivatives of Φ, the relation

$$\frac{\partial^{2m}\Phi}{\partial z^{2m}} = \sum_{n=0}^{\infty} \frac{n!}{(n-2m)!}(z+h)^{n-2m}\phi_n(x,y,t) \tag{29}$$

By applying (6) to the horizontal bottom boundary condition (4), we find that only even integer numbers are acceptable values for n. For Padé(2, 4) Boussinesq equation we take N to be 10, yielding six base functions (ϕ_0, ϕ_2, ϕ_4, ϕ_6, ϕ_8 and ϕ_{10}) to be determined. We first use Equations (27)–(29)

$$\begin{aligned}
\delta^2\hat{\Phi} &= -2d^2\phi_2 + (2d^4 - 12d^2\bar{z}^2)\phi_4 + (-2d^6 + 30d^4\bar{z}^2 - 30d^2\bar{z}^4)\phi_6 \\
&\quad + (2d^8 - 56d^6\bar{z}^2 + 140d^4\bar{z}^4 - 56d^2\bar{z}^6)\phi_8 \\
&\quad + (-2d^{10} + 90d^8\bar{z}^2 - 420d^6\bar{z}^4 + 420d^4\bar{z}^6 - 90d^2\bar{z}^8)\phi_{10} \\
\delta^2\hat{W} &= -24d^2\bar{z}\phi_4 + (60d^4\bar{z} - 120d^2\bar{z}^3)\phi_6 \\
&\quad + (-112d^6\bar{z} + 560d^4\bar{z}^3 - 336d^2\bar{z}^5)\phi_8 \\
&\quad + (180d^8\bar{z} - 1680d^6\bar{z}^3 + 2520d^4\bar{z}^5 - 720d^2\bar{z}^7)\phi_{10}
\end{aligned}$$

to formulate

$$\begin{aligned}
\delta^4\hat{\Phi} &= 24d^4\phi_4 + (-120d^6 + 360d^4\bar{z}^2)\phi_6 \\
&\quad + (504d^8 - 3360d^6\bar{z}^2 + 1680d^4\bar{z}^4)\phi_8 \\
&\quad + (-2040d^{10} + 22680d^8\bar{z}^2 - 25200d^6\bar{z}^4 + 5040d^4\bar{z}^6)\phi_{10} \\
\delta^4\hat{W} &= 720d^4\bar{z}\phi_6 + (-6720d^6\bar{z} + 6720d^4\bar{z}^3)\phi_8 \\
&\quad + (45360d^8\bar{z} - 100800d^6\bar{z}^3 + 30240d^4\bar{z}^5)\phi_{10}
\end{aligned} \tag{30}$$

where $\bar{z} = z + h$. Then, we solve the linear system defined by (30) and (28) for $z = 0$ to obtain the six base functions (ϕ_0, ϕ_2, ϕ_4, ϕ_6, ϕ_8 and ϕ_{10}) with relation to $\hat{\Phi}$, $\hat{W}$, $\delta^2\hat{\Phi}$, $\delta^2\hat{W}$, $\delta^4\hat{\Phi}$ and $\delta^4\hat{W}$. Next, we substitute these six functions into (28) on $z = \eta$ to formulate the relation between $\tilde{\Phi}$ to $\hat{\Phi}$, $\hat{W}$, $\delta^2\hat{\Phi}$, $\delta^2\hat{W}$, $\delta^4\hat{\Phi}$ and $\delta^4\hat{W}$. We can write this relation in a compact form as

$$\tilde{\Phi} = A_{nl}\hat{\Phi} + B_{nl}\hat{W} \tag{31}$$

Equations (31) and (24) can be written in a compact form as

$$\begin{bmatrix} \bar{\bar{A}}_p & -\bar{\bar{B}}_p \\ \bar{\bar{A}}_{nl} & \bar{\bar{B}}_{nl} \end{bmatrix} \begin{bmatrix} \hat{\Phi} \\ \hat{W} \end{bmatrix} = \begin{bmatrix} \mathbf{0} \\ \tilde{\Phi} \end{bmatrix} \tag{32}$$

where $\bar{\bar{A}}_p$, $\bar{\bar{B}}_p$, $\bar{\bar{A}}_{nl}$ and $\bar{\bar{B}}_{nl}$ are the band matrices related to A_p, B_p, A_{nl} and B_{nl}, respectively (see Appendix B). The solution of (32) gives us $\hat{\Phi}$ and $\hat{W}$ for every grid point. This enables

us to find the set of six coefficients (ϕ_0, ϕ_2, ϕ_4, ϕ_6, ϕ_8 and ϕ_{10}) for every grid point. By substituting these coefficients into (28) the vertical profile can be constructed for all the region of calculation leading to the solution of the problem for the nonlinear wave, i.e. finding the vertical velocity on the free surface ($\tilde{W}$). Following Fuhrman and Bingham [9], in order to make the solution of the linear system linear (32) more efficient a rearrangement of the equations can be performed to yield a single banded coefficient matrix.

6. COMPLETING THE METHOD

In the previous sections a new AFD method has been constructed. This method enables us to solve accurately and efficiently the DtN problem for nonlinear waves, that lies in the heart of HOB equations. The final step is to show how the problem is marched in time using the free surface boundary conditions. In order to march η and $\tilde{\Phi}$ in time we use (2) and (3) with a time propagation Runge–Kutta method. The only term that is missing in this stage is $(\nabla\Phi)_{z=\eta}$. Here we should be cautious because we cannot simply apply a FD first derivatives with respect to x and y on $\tilde{\Phi}$. That is because $\tilde{\Phi}$ is the potential on the free surface elevation, which means that it is located on $z=\eta(x,y)$. In order to take the horizontal gradient on the free surface, we apply it to the power series expansion of potential (28) and than substitute $z=\eta$ to receive

$$(\nabla\Phi)_{z=\eta}=\sum_{n=0}^{N}(\eta+h)^n\nabla\phi_n(x,y,t) \tag{33}$$

The base functions in (33) are already computed for every grid point and can be easily differentiated horizontally by applying a FD first derivative operator to them. The AFD method used in Equation (32) gives a high-order accuracy, as show in this paper. The auxiliary computation of $\nabla\phi_n$, which appears in (33) is done by a regular FD approach. Thus, it has lower accuracy for the same stencil width. In order to maintain a uniform overall accuracy we use a double bandwidth in the calculation of $\nabla\phi_n$. The additional computational cost of this operation is negligible.

Note that Equations (2) and (3) are stated in Eulerian formulation. This implies that acquiring $\tilde{\Phi}$ of the next time step should take into account that η has also changed. Applying the chain rule together with Equation (2) yields the relation

$$\tilde{\Phi}_t=(\Phi_t)_{z=\eta}+\tilde{W}\eta_t=(\Phi_t)_{z=\eta}+\tilde{W}(W-\nabla\eta\nabla\Phi)_{z=\eta} \tag{34}$$

By using this relation (34), the dynamic boundary condition (3) takes the form

$$\tilde{\Phi}_t=-g\eta-\tfrac{1}{2}(\nabla\Phi)^2+\tfrac{1}{2}\tilde{W}^2-\tilde{W}\nabla\eta(\nabla\Phi)_{z=\eta},\quad z=\eta \tag{35}$$

which enables us to propagate $\tilde{\Phi}$ to give the potential in the next time step at the appropriate elevation.

7. RESULTS

The previous sections have discussed the derivation of the new AFD method for solving HOB equations. In this section, we provide numerical calculations to verify the performance of the method for nonlinear waves.

As shown by Fenton [14], steady solutions to Stokes waves right up to the steepest wave can be computed with great accuracy using a spectral method based on stream function theory. Here we apply the same technique to solve the AFD Boussinesq Padé(2, 4) approximation and compare to the solution of the exact equations. $\hat{\Phi}$ and $\hat{W}$ are expanded in a Fourier series as

$$\begin{aligned} \hat{\Phi} &= \sum_{j=1}^{n} \frac{B_j}{jk} \cos(jkx), \quad \hat{W} = \sum_{j=1}^{n} C_j \cos(jkx) \\ \hat{\Psi} &= \sum_{j=1}^{n} \frac{C_j}{jk} \cos(jkx) \end{aligned} \tag{36}$$

An algebraic relation between the C_j and B_j coefficients can be found using the linear DtN relation (16). Here, we use Padé(2, 4) in order to approximate this relation as shown in Equation (23). By using (36), (23), (28) and (30) in the free surface conditions at $n+1$ equally spaced grid points from wave crest to wave trough we receive $2n+2$ equations. These equations together with the kinematic constrains are then solved using Newton's method, as in Reference [14]. Figure 10 plots the errors in nonlinear dispersion (wave celerity, e_c), the RMS surface velocities (e_u and e_w) and the RMS surface profile with respect to kh for both the accurate and the standard FD methods. It shows the error of the first three harmonics as well (e_{A_1}, e_{A_2}, e_{A_3}, e_{B_1}, e_{B_2} and e_{B_3}). The wave conditions chosen for calculation are of steepness $ka = 0.05$, 0.10 and 0.15. In all cases $n = 24$ was used and was enough to ensure that $B_n/B_1 \leqslant 10^{-9}$ for both the exact and approximate equations. The distance between two grid points (d) was imposed by the choice of n to be $L/24$. The error metrics used are

$$\begin{aligned} e_w &= \frac{2}{\tilde{W}^e_{\max} L} \sqrt{\int_0^L (\tilde{W}^e - \tilde{W})^2 \, \mathrm{d}x}, \quad e_\eta = \frac{2}{HL} \sqrt{\int_0^L (\eta^e - \eta)^2 \, \mathrm{d}x} \\ e_u &= \frac{2}{\tilde{U}^e_{\max} L} \sqrt{\int_0^L (\tilde{U}^e - \tilde{U})^2 \, \mathrm{d}x}, \quad e_c = \frac{c^e - c}{c^e} \\ e_{A_i} &= \frac{A_i^e - A_i}{A_i^e}, \quad e_{B_i} = \frac{B_i^e - B_i}{B_i^e} \end{aligned} \tag{37}$$

Finally, we applied the method to the problem of a third-order standing wave [15]. Figure 11(a) shows the error bars for the time evolution during 100 periods sampled at one period intervals. Figure 11(b) shows the oscillation of η's error metric defined in (37). This error is comparable to the accuracy of the approximate analytical initial condition.

8. CONCLUSIONS

A new FD method was derived for solving Boussinesq-type equations. Previously, a Padé approximation was found for the dispersion operator in terms of a rational function of the

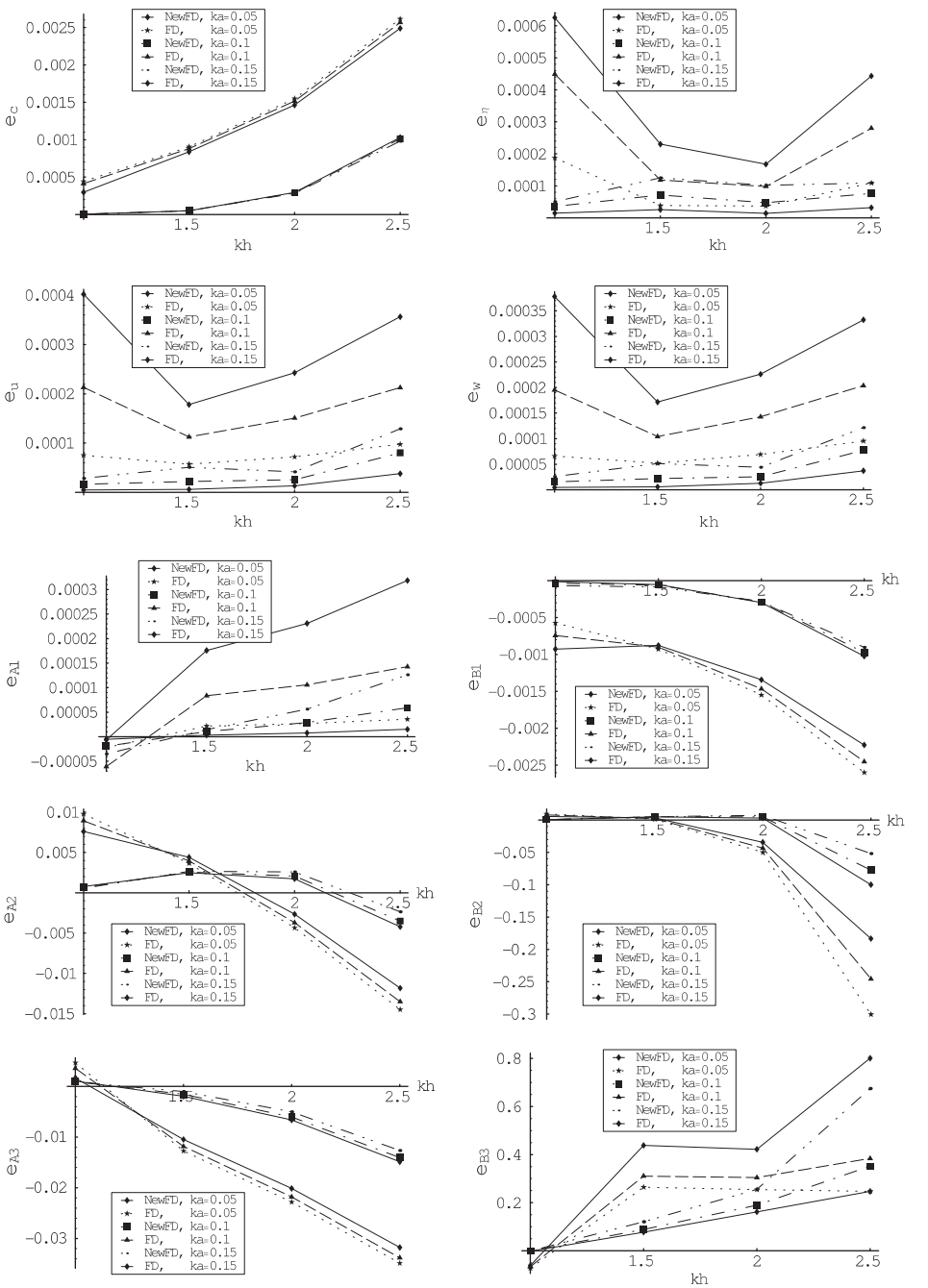

Figure 10. Errors in nonlinear dispersion (e_c), integrated wave profile (e_η), surface velocities (e_u, e_w) and first three harmonics (e_{A_i}, e_{B_i}) computed using both the SFD method and the new AFD method in comparison to the exact equations. See (37) for definitions of the error metrics.

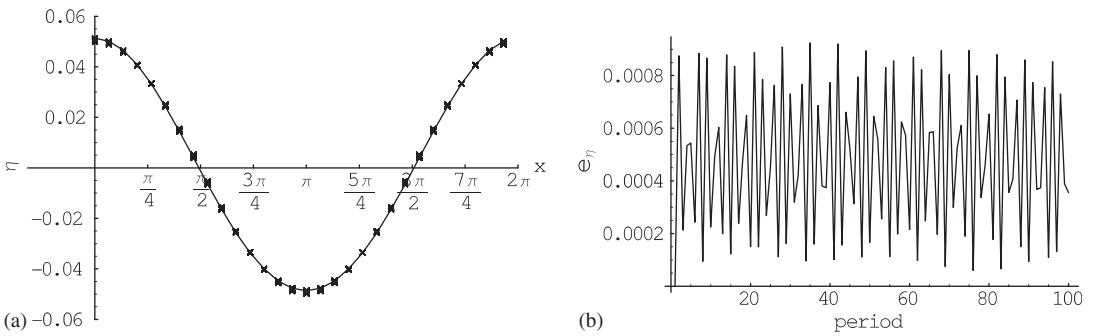

Figure 11. Numerical results for wave parameters of $kh = 2$ and $ka = 0.05$: (a) the error bars for the time evolution during 100 periods sampled at one period intervals; and (b) the oscillation of η's error metric defined in (37).

horizontal gradient operator [16]. Then the numerator and denominator were each evaluated by a finite difference scheme at an order consistent with the order of the derivatives of each. This resulted in relatively large truncation errors. For Padé$(2,4)$ and Padé$(4,6)$ approximations this error added up to the dispersion error and degraded the accuracy of the method. The new method combines these two steps into a single step and finds the Padé expansion directly in terms of the finite difference operator, effectively doubling the order of the finite difference scheme. The linear dispersion relation was studied (including the numerical dispersion) and the method was checked for steady nonlinear waves using the method of Madsen and Agnon [12], which doubles the relative order of the velocity profile. For Padé(4,4) and Padé(6,6), the truncation error and the dispersion error have opposite signs. We found a peculiar phenomenon that holds, for specific values of d/h (grid-size to depth ratio), over a very wide range of wavenumbers: at these values, the total error (the dispersion error plus truncation error) nearly vanishes. This can be utilized to improve the methods' accuracy by choosing that value of d/h for grid spacing. In these cases, choosing the right d/h, the standard HOB method can be used instead of the new method. The approaches presented here can be applied to other problems in which Padé approximants or similar methods are used to approximate high-order differential operators.

APPENDIX A: THE ACCURATE FD STENCILS AND THE STANDARD ONES FOR THE LINEAR CASE

In order to construct the new accurate stencils for $\bar{\bar{A}}_p$ and $\bar{\bar{B}}_p$ in Equation (24) we first need to derive the even powers of the FD operator δ. As shown in Section 3, δ is defined as

$$\delta f(x) = f\left(x + \frac{d}{2}\right) - f\left(x - \frac{d}{2}\right) \tag{A1}$$

Therefore, by applying again the operator to Equation (A1) we get

$$\begin{aligned}
\delta^2 f(x) &= f(x+d) - 2f(x) + f(x-d) \\
\delta^4 f(x) &= f(x+2d) - 4f(x+d) + 6f(x) - 4f(x-d) + f(x-2d) \\
\delta^6 f(x) &= f(x+3d) - 6f(x+2d) + 15f(x+d) - 20f(x) \\
&\quad +15f(x-d) - 6f(x-2d) + f(x-3d)
\end{aligned} \tag{A2}$$

By substituting (A2) into the numerator and the denominator of (23) separately and collecting for all neighbouring grid points, we can construct the two stencils for solving the linear DtN relation (24) with a Padé(2,4) approximation

$$\begin{aligned}
A_p: \quad & \{-15(31d^6h + 112d^2h^5 - 128h^7) \\
& -1920h(d^6 + 7d^2h^4 + 4h^6) \\
& 90(53d^6h + 336d^2h^5 + 128h^7) \\
& -1920h(d^6 + 7d^2h^4 + 4h^6) \\
& -15(31d^6h + 112d^2h^5 - 128h^7)\}
\end{aligned} \tag{A3}$$

$$\begin{aligned}
B_p: \quad & \{23d^8 - 155d^6h^2 - 28d^4h^4 - 720d^2h^6 + 192h^8 \\
& 16(43d^8 - 40d^6h^2 + 217d^4h^4 - 360d^2h^6 - 48h^8) \\
& 6(393d^8 + 265d^6h^2 + 2212d^4h^4 + 2160d^2h^6 + 192h^8) \\
& 16(43d^8 - 40d^6h^2 + 217d^4h^4 - 360d^2h^6 - 48h^8) \\
& 23d^8 - 155d^6h^2 - 28d^4h^4 - 720d^2h^6 + 192h^8\}
\end{aligned} \tag{A4}$$

Taking the Padé(4,6) approximation of (23) gives a more AFD operator representing the DtN relation:

$$\begin{aligned}
G = & \{21(625680d^{16} + 8149680d^{12}h^4 + 6336000d^{10}h^6 + 26611200d^8h^8 + 2027520d^4h^{12}) \\
& + 21(154680d^{16} + 1811880d^{12}h^4 + 834240d^{10}h^6 + 4857600d^8h^8 - 2580480d^6h^{10} \\
& + 337920d^4h^{12} - 245760d^2h^{14})\delta^2 \\
& + 21(7069d^{16} + 61087d^{12}h^4 - 44080d^{10}h^6 + 53680d^8h^8 - 317440d^6h^{10} \\
& - 2816d^4h^{12} - 20480d^2h^{14} + 4096h^{16})\delta^4\} \\
& \div \{-13139280d^{18} - 171143280d^{14}h^4 - 133056000d^{12}h^6 \\
& - 558835200d^{10}h^8 - 42577920d^6h^{12}
\end{aligned}$$

$$
\begin{aligned}
&+(-4343220d^{18}+4379760d^{16}h^2-52311420d^{14}h^4+28440720d^{12}h^6-104227200d^{10}h^8\\
&+240468480d^8h^{10}-10644480d^6h^{12}+19353600d^4h^{14})\delta^2\\
&+(-364392d^{18}+1082760d^{16}h^2-3448536d^{14}h^4+12703320d^{12}h^6+2343264d^{10}h^8\\
&+48142080d^8h^{10}-5999616d^6h^{12}+3225600d^4h^{14}-860160d^2h^{16})\delta^4\\
&+(-5571d^{18}+49483d^{16}h^2+11767d^{14}h^4+537353d^{12}h^6+264712d^{10}h^8\\
&+1210608d^8h^{10}-695808d^6h^{12}-26880d^4h^{14}-71680d^2h^{16}+4096h^{18})\delta^6\}
\end{aligned}
\tag{A5}
$$

Now, as before, by substituting (A2) into the numerator and the denominator of (A5) two stencils can be constructed for the AFD Padé(4,6) approximation.

The SFD DtN relation is acquired by applying Padé approximation to (16) and then approximating the differential operator (∇) using the FD method. The resulting relations for Padé$(2,4)$ and Padé$(4,6)$ are:

$$
\begin{aligned}
\text{SFD, Padé}(2,4):\quad G &= \frac{-420d^2h\delta^2+(35d^2h+40h^3)\delta^4}{420d^4-180d^2h^2\delta^2+(15d^2h^2+4h^4)\delta^4}\\
\text{SFD, Padé}(4,6):\quad G &= \frac{41580d^4h\delta^2+(-3465d^4h-5040d^2h^3)\delta^4+(462d^4h+840d^2h^3+84h^5)\delta^6}{-41580d^6+18900d^4h^2\delta^2+(-1575d^4h^2-840d^2h^4)\delta^4+(210d^4h^2+140d^2h^4+4h^6)\delta^6}
\end{aligned}
\tag{A6}
$$

In linear theory, derivation with respect to x can be regarded as multiplication by ik. This concept together with Equation (21) are used to form the ratios between (23), (A5), (A6) and (16) that are shown in Figures 2–9.

APPENDIX B: THE SOLUTION FOR THE SIX BASE FUNCTIONS

In Section 5, Equations (28) and (30), a linear system relating six base functions (ϕ_0, ϕ_2, ϕ_4, ϕ_6, ϕ_8 and ϕ_{10}) to $\hat{\Phi}$, $\hat{W}$, $\delta^2\hat{\Phi}$, $\delta^2\hat{W}$, $\delta^4\hat{\Phi}$ and $\delta^4\hat{W}$ is presented. Solving the linear system for these base functions on $z=0$ yields,

$$
\begin{aligned}
A_{nl}:\quad &\{(278d^{12}+128h^6\eta^2(2h+\eta)^2(h^2-2h\eta-\eta^2)-511d^{10}(2h^2-2h\eta-\eta^2)\\
&-56d^4h^4(128h^4+256h^3\eta+44h^2\eta^2-84h\eta^3-21\eta^4)\\
&+8d^8(996h^4-352h^3\eta-44h^2\eta^2+132h\eta^3+33\eta^4)\\
&+16d^2h^4(32h^6-32h^5\eta-536h^4\eta^2-464h^3\eta^3-46h^2\eta^4+42h\eta^5+7\eta^6)\\
&+d^6(-9536h^6+10816h^5\eta+4168h^4\eta^2-992h^3\eta^3+62h^2\eta^4+186h\eta^5+31\eta^6))\\
&\frac{\eta^2(2h+\eta)^2}{192d^4(79d^{12}+1029d^8h^4+800d^6h^6+3360d^4h^8+256h^{12})}
\end{aligned}
$$

$$
\begin{aligned}
&(464d^{12} - 16h^6\eta^2(2h+\eta)^2(h^2 - 2h\eta - \eta^2) - 280d^{10}(2h^2 - 2h\eta - \eta^2)\\
&+ d^8(5424h^4 - 608h^3\eta - 76h^2\eta^2 + 228h\eta^3 + 57\eta^4)\\
&+ 7d^4h^4(128h^4 + 256h^3\eta + 404h^2\eta^2 + 276h\eta^3 + 69\eta^4)\\
&+ 4d^6(172h^6 + 1468h^5\eta + 694h^4\eta^2 - 32h^3\eta^3 + 2h^2\eta^4 + 6h\eta^5 + \eta^6)\\
&+ 4d^2h^4(-64h^6 + 64h^5\eta + 232h^4\eta^2 + 256h^3\eta^3 + 134h^2\eta^4 + 42h\eta^5 + 7\eta^6))\\
&\frac{\eta^2(2h+\eta)^2}{6d^4(79d^{12} + 1029d^8h^4 + 800d^6h^6 + 3360d^4h^8 + 256h^{12})}\\
&(2528d^{16} + 128h^6\eta^4(2h+\eta)^4(h^2 - 2h\eta - \eta^2)\\
&+ d^{12}(32928h^4 - 20168h^2\eta^2 - 20168h\eta^3 - 5042\eta^4)\\
&+ d^{10}(25600h^6 + 25256h^4\eta^2 - 31570h^2\eta^4 - 18942h\eta^5 - 3157\eta^6)\\
&+ 16d^2h^4\eta^2(2h+\eta)^2\\
&(160h^6 - 160h^5\eta - 440h^4\eta^2 - 528h^3\eta^3 - 342h^2\eta^4 - 126h\eta^5 - 21\eta^6)\\
&- d^6\eta^2(2h+\eta)^2\\
&(4160h^6 + 66240h^5\eta + 31000h^4\eta^2 - 1696h^3\eta^3 + 106h^2\eta^4 + 318h\eta^5 + 53\eta^6)\\
&+ 8d^4h^4(1024h^8 - 3584h^6\eta^2 - 10752h^5\eta^3 - 22736h^4\eta^4\\
&- 27552h^3\eta^5 - 17528h^2\eta^6 - 5544h\eta^7 - 693\eta^8)\\
&+ 8d^8(13440h^8 - 30256h^6\eta^2 - 26544h^5\eta^3 - 3388h^4\eta^4 - 1624h^2\eta^6 - 696h\eta^7 - 87\eta^8))\\
&\frac{1}{32d^4(79d^{12} + 1029d^8h^4 + 800d^6h^6 + 3360d^4h^8 + 256h^{12})}\\
&A_{nl}(2)\\
&A_{nl}(1)\}
\end{aligned}
$$

$$
\begin{aligned}
B_{nl}: \quad &\{(140d^{14} + 192h^8\eta^3(2h+\eta)^3 + d^{12}(-1924h^2 + 534h\eta + 267\eta^2)\\
&+ 5d^{10}(1440h^4 - 1342h^3\eta - 551h^2\eta^2 + 120h\eta^3 + 30\eta^4)\\
&+ 80d^2h^6\eta(32h^5 + 208h^4\eta + 120h^3\eta^2 - 60h^2\eta^3 - 54h\eta^4 - 9\eta^5)\\
&+ 4d^4h^4(3840h^6 + 5120h^5\eta - 4960h^4\eta^2 - 7576h^3\eta^3 - 1964h^2\eta^4 - 42h\eta^5 - 7\eta^6)\\
&+ d^8(-43648h^6 + 14048h^5\eta + 824h^4\eta^2 - 6016h^3\eta^3 - 1274h^2\eta^4 + 138h\eta^5 + 23\eta^6)\\
&- 5d^6h^2(512h^6 + 11072h^5\eta + 4896h^4\eta^2 - 392h^3\eta^3 + 212h^2\eta^4 + 186h\eta^5 + 31\eta^6))
\end{aligned}
$$

$$
\begin{aligned}
&\frac{\eta^2(2h+\eta)^2}{2880d^4(79d^{12}h+1029d^8h^5+800d^6h^7+3360d^4h^9+256h^{13})}\\
&(-880d^{14}+48h^8\eta^3(2h+\eta)^3+8d^{12}(898h^2-318h\eta-159\eta^2)\\
&-5d^{10}(4176h^4-2048h^3\eta-676h^2\eta^2+348h\eta^3+87\eta^4)\\
&+40d^2h^6\eta(64h^5+56h^4\eta+96h^3\eta^2+114h^2\eta^3+54h\eta^4+9\eta^5)\\
&+d^4h^4(3840h^6+5120h^5\eta+28640h^4\eta^2+24344h^3\eta^3\\
&+3916h^2\eta^4-1302h\eta^5-217\eta^6)\\
&+d^8(69488h^6-34288h^5\eta-13144h^4\eta^2+3656h^3\eta^3+484h^2\eta^4-258h\eta^5-43\eta^6)\\
&+5d^6h^2(5248h^6+14368h^5\eta+4572h^4\eta^2-2548h^3\eta^3-557h^2\eta^4+48h\eta^5+8\eta^6))\\
&\frac{-\eta^2(2h+\eta)^2}{2880d^4(79d^{12}h+1029d^8h^5+800d^6h^7+3360d^4h^9+256h^{13})}\\
&18960d^{16}(2h+\eta)+35160d^{14}\eta(2h+\eta)^2+192h^8\eta^4(2h+\eta)^5\\
&+80d^2h^6\eta^2(2h+\eta)^3(80h^4+108h^2\eta^2+108h\eta^3+27\eta^4)\\
&+d^{12}(493920h^5+182704h^4\eta+100840h^3\eta^2+231580h^2\eta^3+123822h\eta^4+20637\eta^5)\\
&+5d^6h^2\eta(2h+\eta)^2\\
&(28160h^6+80320h^5\eta+66336h^4\eta^2+26600h^3\eta^3+7180h^2\eta^4+318h\eta^5+53\eta^6)\\
&+15d^{10}(25600h^7+119424h^6\eta+101304h^5\eta^2+23828h^4\eta^3\\
&+6314h^3\eta^4+7063h^2\eta^5+2576h\eta^6+322\eta^7)\\
&+d^8(1612800h^9+2185728h^8\eta+2940800h^7\eta^2+2679840h^6\eta^3+1169280h^5\eta^4\\
&+215824h^4\eta^5+27840h^3\eta^6+15270h^2\eta^7+3930h\eta^8+393\eta^9)\\
&+4d^4h^4(30720h^9+15360h^8\eta+35840h^7\eta^2+183680h^6\eta^3\\
&+304416h^5\eta^4+243600h^4\eta^5\\
&+109200h^3\eta^6+30240h^2\eta^7+5530h\eta^8+553\eta^9)\\
&\frac{\eta}{480d^4(79d^{12}h+1029d^8h^5+800d^6h^7+3360d^4h^9+256h^{13})}
\end{aligned}
$$

$B_{nl}(2)$

$B_{nl}(1)\}$

Here, $A_{nl}(1)$, $A_{nl}(2)$, $B_{nl}(1)$ and $B_{nl}(2)$ represent the first and second terms in the numerical stencils for A and B, respectively. This results from the symmetry of these two stencils.

REFERENCES

1. Boussinesq J. Théorie des ondes et des remous qui se propagent le long d'un canal rectangulaire horizontal, en comuniquant au liquide contenu dans ce canal des vitesse sensiblement pareilles de la surface au fond. *Journal de Mathematiques Pures et Appliquees* 1872; **17**(2):55–108.
2. Peregrine DH. Long waves on a beach. *Journal of Fluid Mechanics* 1967; **27**:815–827.
3. Bingham HB, Agnon Y. A fully dispersive Fourier–Boussinesq method for nonlinear surface waves. *European Journal of Mechanics B. Fluids* 2004; **24**(2):255–274.
4. Madsen PA, Schäffer HA. A review for Boussinesq-type equations for gravity waves. In *Advances of Coastal and Ocean Engineering*, vol. 5, Liu P (ed.). World Scientific: Singapore, 1999; 1–95.
5. Nwogu O. Alternative form of Boussinesq equations for nearshore wave propagation. *Journal of Waterway, Port, Coastal and Ocean Engineering* 1993; **119**:618–638.
6. Agnon Y, Madsen PA, Schäffer HA. A new approach to high-order Boussinesq models. *International Journal of Fluid Mechanics* 1999; **399**:319–333.
7. Kennedy AB, Kirby JT, Gobbi MF. Simplified higher order Boussinesq equations. 1: linear considerations. *Coastal Engineering* 2002; **44**(3):205–229.
8. Lynett PJ, Liu PL-F. A two-layer approach to water wave modeling. *Proceedings of the Royal Society of London, Series A* 2004; **460**:2637–2669.
9. Furman DR, Bingham HB. Numerical solution of fully non-linear and highly dispersive Boussinesq equations in two horizontal dimensions. *International Journal for Numerical Methods in Fluids* 2004; **44**:231–255.
10. Kirby JT. Boussinesq models and applications to nearshore wave propagation, surfzone processes and wave-induced currents. In *Advances in Coastal Modeling*, Lakhan VC (ed.). Elsevier: Amsterdam, 2003; 1–41.
11. Harari I, Turkel E. Accurate finite difference methods for time-harmonic wave propagation. *Journal of Computational Physics* 1995; **119**:252–270.
12. Madsen PA, Agnon Y. Accuracy and convergence of velocity formulations for water waves in framework of Boussinesq theory. *Journal of Fluid Mechanics* 2003; **477**:285–319.
13. Rayleigh L. On waves. *Philosophical Magazine* 1876; **5**(1):257–279.
14. Fenton JD. The numerical solution of steady water wave problem. *Computational Geoscience* 1988; **14**(3): 357–368.
15. Okamura M. Resonant standing waves on water of uniform depth. *Journal of the Physical Society of Japan* 1997; **66**(12):3801–3808.
16. Madsen PA, Murray R, Sorensen OR. A new form of the Boussinesq equations with improved linear dispersion characteristics. *Coastal Engineering* 1991; **15**:371–388.

